Electronic Supplementary Information

Diameter-optimized high-order waveguide nanorods for fluorescence enhancement applied in ultra-sensitive bioassays

Baosheng Du,[a,c] Chengchun Tang,[b] Dan Zhao,[f] Hong Zhang,[a] Dengfeng Yu,[a,c] Miao Yu,[c] Krishna C. Balram,[d] Henkjan Gersen,[e] Bin Yang,[a] Wenwu Cao,[a] Changzhi Gu,[b] Flemming Besenbacher,*[g] Junjie Li*[b] and Ye Sun*[a]*

[a] *Condensed Matter Science and Technology Institute, School of Instrumentation Science and Engineering,, Harbin Institute of Technology, Harbin 150080, China. E-mail: sunye@hit.edu.cn.*

[b] *Beijing National Laboratory for Condensed Matter Physics, Institute of Physics, Chinese Academy of Sciences, Beijing 100190, China. E-mail: jjli@iphy.ac.cn.*

[c] *State Key Laboratory of Urban Water Resource and Environment, School of Chemistry and Chemical Engineering, Harbin Institute of Technology, Harbin 150001, China. E-mail: miaoyu_che@hit.edu.cn.*

[d] *QET Labs, Department of Electrical & Electronic Engineering, University of Bristol, Bristol, BS8 1UB, United Kingdom*

[e] *Nanophotonics and Nanophysics Group, H. H. Wills Physics Laboratory, University of Bristol, Bristol, BS8 1TL, United Kingdom*

[f] *National Key Laboratory of Tunable Laser Technology, Harbin Institute of Technology, Harbin 150001, China*

[g] *iNANO and Department of Physics and Astronomy, Aarhus University, Aarhus 8000, Denmark. E-mail: fbe@inano.au.dk*

**Fluorescence enhancement properties of the NRs without the Au layer**

ZnO NR arrays were fabricated using the same procedure and method, whist the ZnO seed layer was deposited directly onto the Si substrate without pre-depositing an Au layer. The obtained six types of ZnO-NRs arrays are named as '*Z1*', '*Z2*', '*Z3*', '*Z4*', '*Z5*', and '*Z6*', growing from the aperture arrays with the same size as the *AZ* samples. The resulting ZnO NRs in each array have approximately the same diameter, height, and lateral arrangement to those on the substrate with the Au layer. The fluorescent images and fluorescence-intensity distribution of this new series of samples treated by R6G solutions at various concentrations are presented in Fig. S6. In absence of the Au layer, although the FE of all NRs arrays was lower that of the *AZ* samples, the *Z3* arrays with an average *d* of ~230 nm still presented the best fluorescence detection at all the given R6G concentrations, which is in good agreement with the performance of its associated *AZ3*. FDTD simulations were also performed for this case (Fig. S7). Similar to the *AZ* results, the NR with *d* of 230 nm also presents the strongest simulated evanescent field and $E_{\text{interface}}$, confirming that the *d*-dependent high-order waveguide modes plays a key role in the FE properties of ZnO NRs.

Comparing the fluorescence intensity measured from the *AZ3* and *Z3* treated by R6G solutions at various concentrations (1 μM, 1 nM, and 1 pM), the Au layer was confirmed to enhance the detected fluorescence signal effectively (Fig. 3a). For instance, the fluorescence intensity of *AZ3* treated by 1 pM R6G solution was even stronger than that of *Z3* treated by 1 nM R6G. As a result, a super low LOD of 0.1 fM for R6G probe detection was achieved from *AZ3* (Fig. 2a), which is two orders improved compared with the LOD of the corresponding NRs arrays without the Au layer (10 fM, Fig. S6a−b). Since the thicknesses of the ZnO seed layer and the remaining PMMA layer are

much larger than the required metal-fluorophore coupling distance (usually < 20 nm),[S1] metal enhanced fluorescence effect does not influence the FE properties of *AZ* arrays. This is further confirmed by the nearly the same fluorescence lifetimes of the R6G on the ZnO NR in the presence/absence of the Au layer (Fig. S9). It is worthy of mention that, the Au-covered Si showed a much higher diffuse reflectance than the bare Si substrate for excitation with wavelength > 500 nm (Fig. S9). Therefore, the Au layer may promote FE properties of the NR arrays in two ways: (1) to reduce the absorption of the Si substrate upon both the excitation and the emission light; (2) to enhance waveguiding properties of the ZnO NRs by providing a reflecting mirror.[S2] As confirmed by the FDTD simulations (Fig. S7), the evanescent field of the NRs with the Au layer shows ~1 fold enhancement, indicating the significant contribution of the Au layer to the high FE performance.

To further evaluate the FE performance of the AZ NR arrays, FE properties of the *AZ3* and *Z3* samples together with the PMMA layer, the ZnO seed layer, and a glass substrate were compared (treated by 1 µM R6G and measured under the same conditions). As seen in Fig. 3b, the detected fluorescence intensity of R6G on *AZ3* was ~2 fold as that on *Z3*, ~20 fold as that on the ZnO seed layer and PMMA layer. Notably, *AZ3* resulted in ~300 fold enhancement of the detected fluorescence intensity in comparison to the glass substrate, which is higher than all the reported results of the ZnO-based FE platform.[S3,S4]
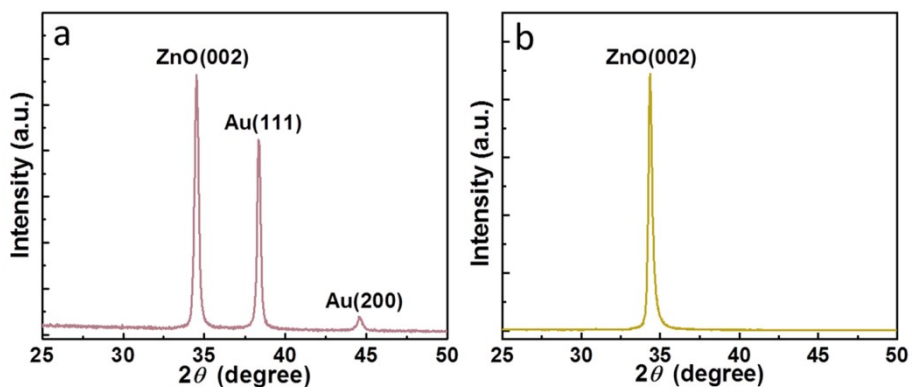
Fig. S1 X-ray diffraction pattern of ZnO seed layer grown on (a) Au layer-coated Si substrate and (b) bare Si substrate.
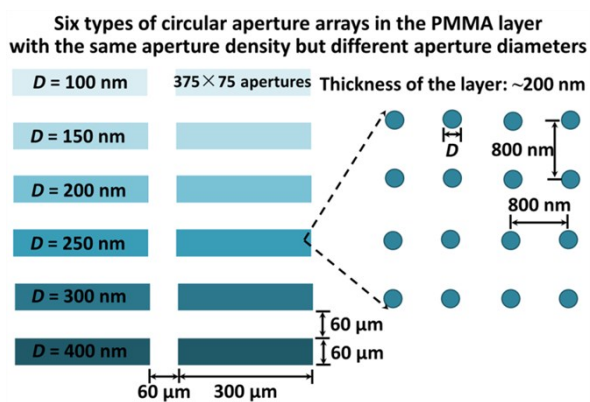
Fig. S2 The geometries and parameters of the aperture arrays in the PMMA layer
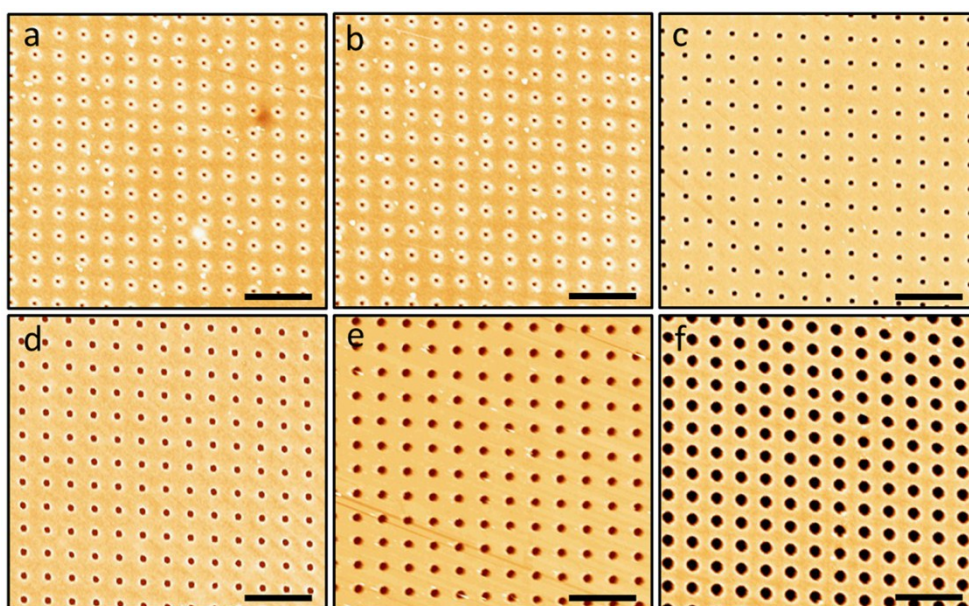

Fig. S3 Atomic force microscopy images of the circular holes formed in the PMMA layer with the target diameters of (a) ~100 nm, (b) ~150 nm, (c) ~200 nm, (d) ~250 nm, (e) ~300 nm, and (f) ~400 nm, respectively. The scale bars are 2 μm.
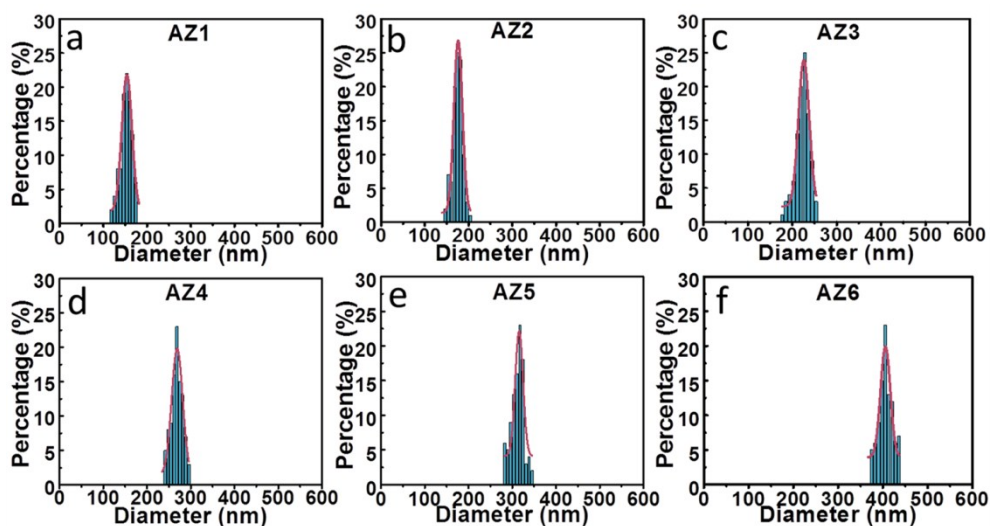
Fig. S4 Diameter distribution of the ZnO nanorods spouted out from the six types of the holes. The average diameters are (a) ~150 nm, (b) ~180 nm, (c) ~230 nm, (d) ~270 nm, (e) ~320 nm, and (f) ~410 nm, respectively.

Table S1 The average diameter, estimated surface area of a single *AZ* NR (*A*), measured fluorescence intensity (*I*), and normalized intensity (*I/A)* of *AZ1*–*AZ*6 arrays, treated by 1 μM R6G solution.

| Array	Average diameter (nm)	A (μm^2)	I (a.u.)	I/A (μm^{-2})
AZ1	~150	~0.68	~400	~590
AZ2	~180	~0.82	~500	~610
AZ3	~230	~0.98	~2000	~2040
AZ4	~270	~0.99	~1100	~1110
AZ5	~320	~1.06	~1000	~940
AZ6	~410	~1.42	~1100	~770
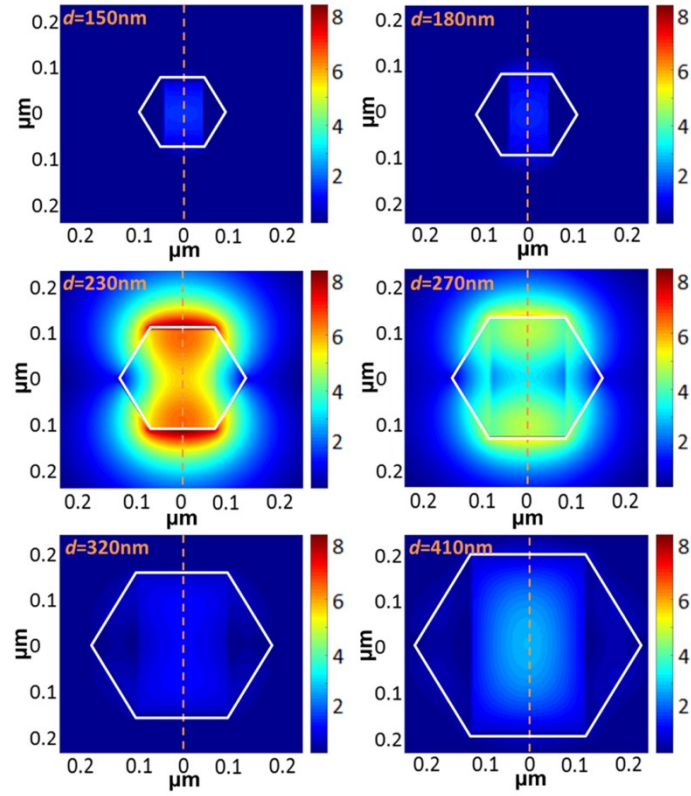
Fig. S5 The |E| distribution on an *x-y* plane of the *AZ* NRs with different *d*.

Table S2 The calculated average $E_{interface}$ values of the NRs with the same *d* of 230 nm but different NR heights of 1.5, 1.4, 1.3, 1.2, 1.1, and 1.0 μm.

NR Height	1.5 μm	1.4 μm	1.3 μm	1.2 μm	1.1 μm	1.0 μm
Average $E_{interface}$	6.42	6.21	6.23	6.19	6.14	6.07
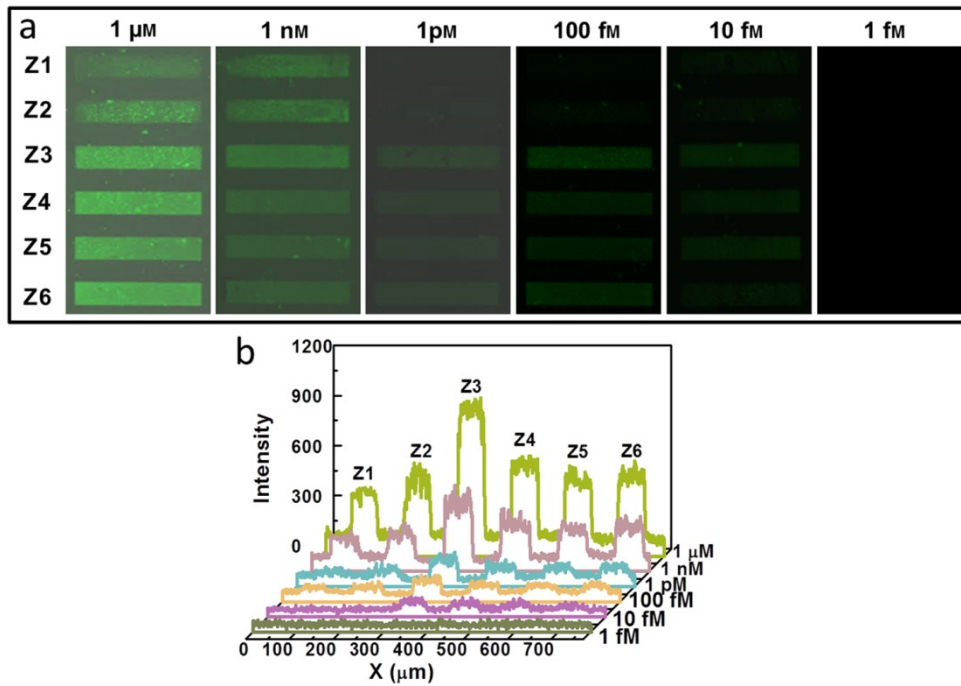
Fig S6. (a) Fluorescent images and (b) fluorescence-intensity distribution of the Si/ZnO NRs samples treated by R6G solutions with different concentrations.
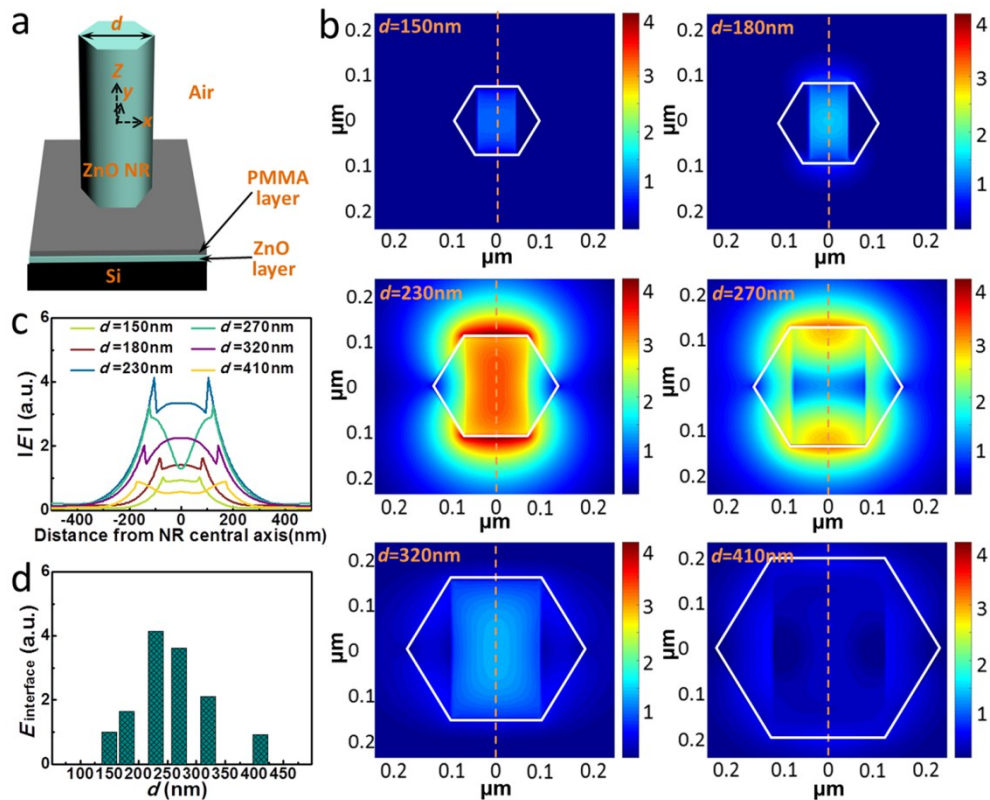
Fig. S7 (a) Configuration and (b) |E| distribution on an x-y plane of the Z NRs with different d. (c) |E| along the y–axis and (d) the evanescent field at the ZnO/air interface $E_{interface}$ of the Z NRs with d of 150, 180, 230, 270, 320, and 410 nm.
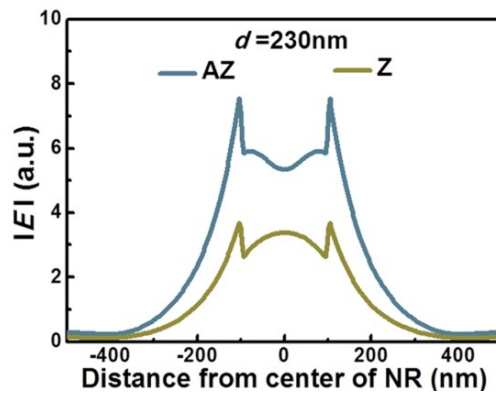
Fig. S8 |*E*| along the *y*–axis of the *AZ* and *Z* NRs with *d* of 230 nm.
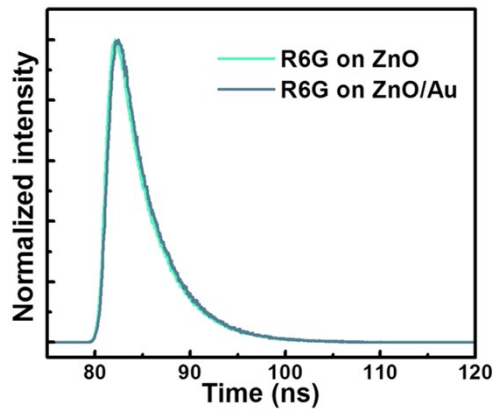
Fig. S9 Time-resolved fluorescence spectra of R6G on the ZnO NRs in the presence/absence of the Au layer.
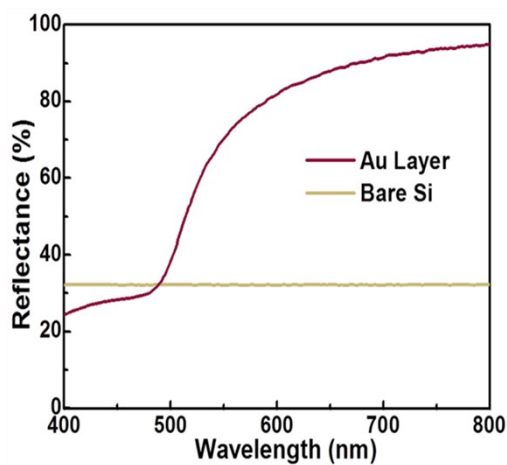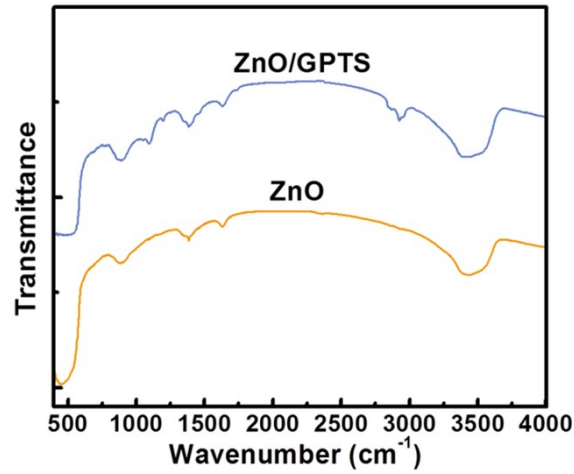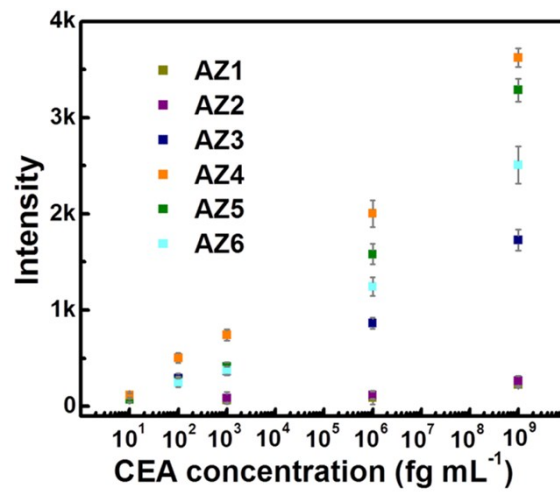

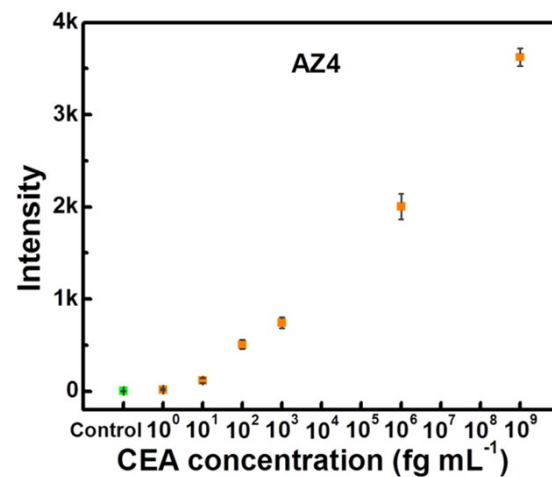**Fig. S10** Diffuse reflectance of the Au layer and the Si substrate.

Fig. S11 FTIR spectra of the pristine ZnO NRs and the GPTS-modified ZnO NRs.

Fig. S12 Fluorescence intensity measured from the *AZ1*, *AZ2*, *AZ3*, *AZ4*, *AZ5* and *AZ6* arrays as a function of CEA concentration.

Fig. S13 Fluorescence intensity measured from the *AZ4* arrays as a function of CEA concentration.
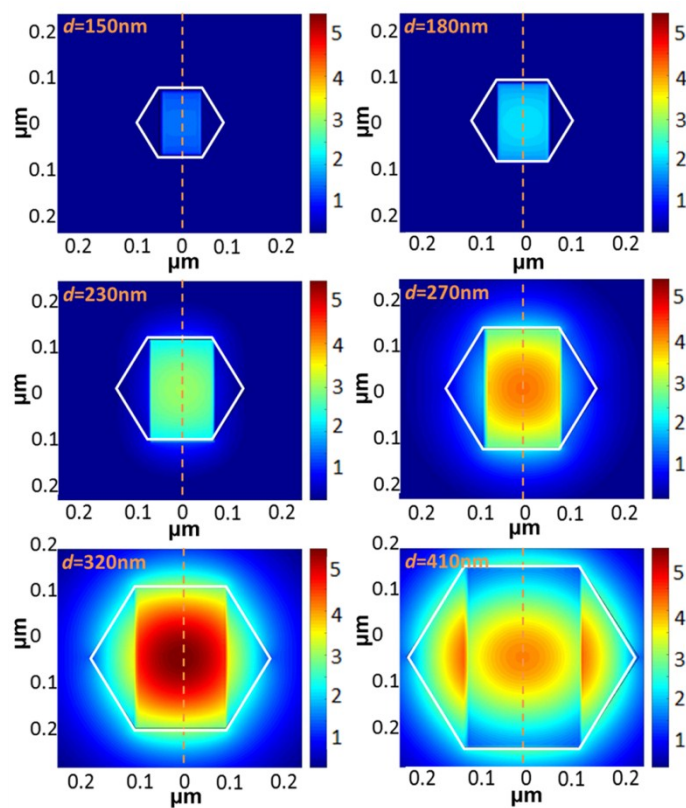
Fig. S14 |*E*| distribution on an *x-y* plane of the *AZ* NRs with surrounding medium of *n* =1.4.

References

S1 J. Hahm, *J Nanosci Nanotechnol.*, 2014, **14**, 475–486.

S2 Y. Yin, Y. Sun, M. Yu, X. Liu, T. Jiang, B. Yang, D. Liu, S. Liu and W. Cao, *Sci. Rep.*, 2015, **5**, 8152.

S3 C. Liu, F. Meng, W. Zheng, T. Xue, Z. Jin, Z. Wang and X. Cui, *Sens. Actuators B*, 2016, **228**, 231–236.

S4 T. Wang, A. Centeno, D. Darvill, J. S. Pang, M. P. Ryan and F. Xie, *Phys. Chem. Chem. Phys.*, 2018, **20**, 14828–14834.